




Article

Toxicological Profiling of Onion-Peel-Derived Mesoporous Carbon Nanospheres Using In Vivo *Drosophila melanogaster* Model

Vinay S. Bhat ^{1,2,†} , Avinash Kundadka Kudva ^{3,†} , Harshitha Venkatesh Naik ⁴, Reshmi G. ⁴, Shamprasad Varija Raghu ^{4,*}, Paola De Padova ^{5,6,*} and Gurusurthy Hegde ^{7,8,*} 

- ¹ Centre for Nano-Materials & Displays (CND), B.M.S. College of Engineering, Bull Temple Road, Bengaluru 560019, Karnataka, India; s.vinaybhat@gmail.com
- ² Department of Materials Science, Mangalore University, Mangalagangothri 574199, Karnataka, India
- ³ Department of Biochemistry, Mangalore University, Mangalagangothri 574199, Karnataka, India; avinash.kudva@gmail.com
- ⁴ Neurogenetics Lab, Department of Applied Zoology, Mangalore University, Mangalagangothri 574199, Karnataka, India; harshithasuvarnavn@gmail.com (H.V.N.); rashmigatty20@gmail.com (R.G.)
- ⁵ Consiglio Nazionale delle Ricerche-ISM, Via Fosso del Cavaliere 100, 00133 Roma, Italy
- ⁶ INFN-LNF, Via Enrico Fermi 54, 00044 Frascati, Italy
- ⁷ Centre for Advanced Research and Development (CARD), CHRIST (Deemed to be University), Hosur Rd, Bhavani Nagar, S.G. Palya, Bengaluru 560029, Karnataka, India
- ⁸ Department of Chemistry, CHRIST (Deemed to be University), Hosur Rd, Bhavani Nagar, S.G. Palya, Bengaluru 560029, Karnataka, India
- * Correspondence: shamprasadvrijaraghu@gmail.com (S.V.R.); paola.depadova@artov.ism.cnr.it (P.D.P.); murthyhegde@gmail.com (G.H.)
- † These authors contributed equally to this work.



Citation: Bhat, V.S.; Kudva, A.K.; Naik, H.V.; G., R.; Raghu, S.V.; De Padova, P.; Hegde, G. Toxicological Profiling of Onion-Peel-Derived Mesoporous Carbon Nanospheres Using In Vivo *Drosophila melanogaster* Model. *Appl. Sci.* **2022**, *12*, 1528. <https://doi.org/10.3390/app12031528>

Academic Editors: Marilena Carbone and Yuri K. Gun'ko

Received: 15 December 2021

Accepted: 27 January 2022

Published: 31 January 2022

Publisher's Note: MDPI stays neutral with regard to jurisdictional claims in published maps and institutional affiliations.



Copyright: © 2022 by the authors. Licensee MDPI, Basel, Switzerland. This article is an open access article distributed under the terms and conditions of the Creative Commons Attribution (CC BY) license (<https://creativecommons.org/licenses/by/4.0/>).

Featured Application: The lower or less toxic effects of CNSs in an in vivo genetic model such as *Drosophila melanogaster* support its possible use in biological applications such as drug carriers and others.

Abstract: Toxicological profiling of the novel carbon materials has become imperative, owing to their wide applicability and potential health risks on exposure. In the current study, the toxicity of mesoporous carbon nanospheres synthesized from waste onion peel was investigated using the genetic animal model *Drosophila melanogaster*. The survival assays at different doses of carbon nanoparticles suggested their non-toxic effect for exposure for 25 days. Developmental and behavioral defects were not observed. The biochemical and metabolic parameters, such as total antioxidant capacity (TAC), protein level, triglyceride level, and glucose, were not significantly altered. The neurological toxicity as analyzed using acetylcholinesterase activity was also not altered significantly. Survival, behavior, and biochemical assays suggested that oral feeding of mesoporous carbon nanoparticles for 25 days did not elicit any significant toxicity effect in *Drosophila melanogaster*. Thus, mesoporous carbon nanoparticles synthesized from waste onion peel can be used as beneficial drug carriers in different disease models.

Keywords: carbon nanospheres; *Drosophila*; nanotoxicity; acetylcholine; total antioxidant capacity (TAC)

1. Introduction

Carbon, a vital element in nature, is a primary component in all life forms. The uniqueness of the element arises due to the number and variety of ways in which it can bond, leading to numerous carbonaceous structures with distinctive properties [1]. Along with traditionally known amorphous and crystalline carbons, newer allotropes such as graphene, carbon nanotubes (CNTs), fullerenes, and other various forms have contributed

immensely to the development of application-oriented research. Nanomaterials based on carbon are the most engrossing part of nanotechnology. However, producing the desired form of carbon via synthetic methods is still not economically viable for many applications. In this context, biomass carbonization has become a very attractive option for the targeted production of carbon forms. The surface chemistry associated with these carbon materials has attracted widespread research efforts devoted to such carbon production (activated and non-activated) [2,3], characterizations, surface modifications, and use [4–7]. The unique physicochemical properties of carbon nanoforms make them ideal materials for catalysis, adsorption, hydrogen storage, electrochemical sensors [8], and energy storage devices [9–12]. The inimitable features of carbon allotropes have also been widely exploited in diverse biological applications, including biosensing, drug delivery, tissue engineering, imaging, cancer therapy, and antimicrobial agents [13]. The widespread utilization of carbon nanoforms has had a profound impact on the advancement of nanotechnology; graphene, CNTs, and fullerenes have also elicited immunological effects [14].

Numerous *in vitro* studies recently have highlighted the cellular toxicity of carbon-based materials [13]. The carbon materials were found to induce oxidative stress and trigger the generation of reactive oxygen species (ROS) [15]. Recent studies have also shed light on lysosomal dysfunction as an emerging factor in nanomaterial toxicity [16]. The multi-walled carbon nanotubes (MWCNTs) were shown to induce necrosis and trigger cell apoptosis [17]. Studies have shown that the physical properties of carbon nanomaterials play a significant role while eliciting cytotoxic responses. One of the studies on MWCNTs of differing length observed differing effects on macrophages. CNTs with an average length of 825 nm elicited stronger inflammation than CNTs with an average length of 220 nm [18]. Another study that focused on the size of carbon nanomaterials concluded that the smaller-sized MWCNTs appeared to be more toxic than larger aggregates [19]. The geometry of carbon nanomaterials was also found to have a profound impact on cytotoxic and immunological responses. In a study involving MWCNTs, the authors found elongated MWCNTs to be more toxic than spherical-shaped carbon nanoparticles [13]. Interestingly, functionalized carbon nanomaterials were observed to be less toxic than nonfunctionalized counterparts. It is believed that functionalization causes disruptions and defects in the carbon framework, which could reduce the toxicity of functionalized carbon nanomaterials [20]. *In vivo* studies on various carbon nanomaterials have also shed light on the toxicological effects of such materials. In one such study, the sixteen-hour exposure of rod-like CNTs via pharyngeal aspiration in mice induced strong neutrophil influx into the lungs, with enhanced cytokines and chemokines [21]. It was found that the inhalation of SWCNTs could up-regulate numerous proteins, resulting in an inflammatory response, playing a role in airway hyperreaction, airflow obstruction, and granuloma, in mice [22]. Such local exposure of carbon nanomaterials not only induces local adverse effects but there is also evidence suggesting a systematic inflammatory response [23]. Similar to *in vitro* studies, *in vivo* studies also found a direct relation between the toxicity of nanomaterials and their physical properties (size, shape, functionalization, etc.).

Nanomaterials and carbon-based materials are today finding wide applicability due to their unique physico-chemical features. This exposure, however, has raised concerns regarding the health hazards associated with their use. At the outset, during the development of any nanomaterials or carbon nanomaterials, it is necessary to evaluate the potential toxic effects. Hence, toxicological profiling of the synthesized novel carbon materials becomes imperative. *Drosophila melanogaster* is widely used as a model organism to study the toxic effects of different nanoparticles [24–27]. The common biological and physiological properties among mammals and *Drosophila* make such studies more relevant. *Drosophila* also shares around 75% sequence similarity with genes causing different diseases in humans [28]. The different genetic tool kits to regulate gene expression levels in *Drosophila* research make them a versatile model organism for various biological studies [29–31]. In the current study, wild-type *Drosophila melanogaster* was used to evaluate the toxicity of mesoporous carbon nanoparticles at different concentrations (10, 100, and 1000 µg/mL). The current *in vivo*

studies demonstrate that mesoporous carbon nanospheres (CNSs) synthesized from waste onion peel are non-toxic at a lower concentration. Thus, they could be a potential drug carrier to mitigate biological defects in different animal disorders.

2. Materials and Methods

2.1. Synthesis and Characterization of Mesoporous Carbon Nanospheres

Waste onion peels were used as a precursor for synthesizing mesoporous carbon nanospheres (CNSs) via pyrolysis at various temperatures (500 to 1000 °C) under an inert atmosphere in a quartz tube furnace. The dried and powdered onion peels were sieved using 60 µm mesh. Then, ~10 g of these were used as precursors and kept for carbonization at 500, 600, 700, 800, 900, and 1000 °C. The pyrolyzed carbon residues were labeled as CNS500, CNS600, CNS700, CNS800, CNS900, and CNS1000, each representing the temperature at which they were synthesized. The morphology of the prepared CNSs was further characterized by field emission scanning microscopy (FESEM; JEOL, JSM-7100F) coupled with energy-dispersive X-ray spectroscopy (EDS); the degree of disorder in the carbon lattice was understood from Raman spectroscopy (HORIBA); functional groups present in CNSs were established by Fourier transform infrared spectroscopy (FTIR; PerkinElmer Spectrum 100), and the porosity was determined from N₂ adsorption/desorption isotherms (BELSORP-max, Microtrac).

2.2. Feeding Experiments

Flies: The wild-type *Drosophila melanogaster* (Canton-S) flies were used. They were maintained at 25 °C, 60–70% humidity, and a 12:12 light–dark cycle on standard fly food.

For all the experiments, the flies were fed with three different concentrations (10, 100, and 1000 µg/mL doses) of CNS500, CNS600, CNS700, CNS800, CNS900, and CNS1000 mesoporous carbon nanoparticles. Different concentrations of CNSs were mixed with 5% yeast solution and sonicated periodically to obtain a uniform dispersion. The mixture was added to fresh food vials and kept at room temperature for 24 h. The next day, 50 female and 50 male flies were transferred to the nanoparticle-treated vials. These flies were further used for survival, behavioral, developmental, biochemical, and neurological assays. In all the assays, the flies fed with 5% yeast without CNSs were used as a control. The flies were transferred into new CNS-treated vials every 3–4 days to prevent flies from sticking to old media.

2.3. Morphological Observations

Both male and female flies from the control and treatment groups were observed for any morphological changes after feeding on nanoparticles for 25 days.

2.4. Survival Assay

A survival assay was performed to assess the effect of CNS (CNS500, CNS600, CNS700, CNS800, CNS900, and CNS1000) exposure of flies to different doses. Briefly, 50 male and 50 female flies were maintained separately in control as well as CNS (CNS500, CNS600, CNS700, CNS800, CNS900, and CNS1000) food vials. The mortality rate was analyzed by counting the dead flies in each vial daily for 25 days. The flies that escaped and stuck to the food were excluded from the count. A survival curve was plotted using GraphPad Prism 6 for analyzing the significant difference between the treatment groups.

As the survival assay did not show a significant level of mortality for different concentrations of CNSs (CNS500, CNS600, CNS700, CNS800, CNS900, and CNS1000), only the flies subjected to the highest concentration were used for climbing and other biochemical assays.

2.5. Climbing Assay

First, 25-day-old control and CNS-treated flies were transferred to a 25-cm-long tube containing a mark at 20 cm. The two ends of the tube were closed using parafilm, with minute holes for air exchange. The flies were tapped down 2–3 times to ensure that all the

flies were at the bottom of the tube. The flies were then allowed to climb for 20 cm, and the number of flies that crossed the mark in 1 min was counted. This procedure was repeated three times, and a percentage value was used for plotting the final graph.

2.6. Estimation of Acetylcholinesterase (AChE) Activity

AChE activity in adult flies (25 flies/group) exposed to CNSs (CNS500, CNS600, CNS700, CNS800, CNS900, and CNS1000) along with food for 25 days was estimated using Ellman's method [32] with some modifications [26]. Briefly, 25 male and female flies were separately homogenized in 500 μ L of 0.1 M sodium phosphate buffer containing 0.15 M KCl (pH 7.4) and centrifuged at 6000 rpm for 10 min at 4 $^{\circ}$ C. Then, the supernatant was separated, and 200 μ L of supernatant was added to a reaction mixture containing 650 μ L of 0.1 M sodium phosphate buffer (pH 7.4), 200 μ L of 10 mM 5,5'-dithiobis-2-nitrobenzoic acid, and 20 μ L of 0.075 M acetylthiocholine iodide. All the components were mixed well and the change in absorbance per min was recorded at 412 nm to calculate the AChE activity.

2.7. Total Antioxidant Capacity (TAC)

The TAC assay was performed as per the previously described method [33]. This test is used to gauge the inhibition of the reducing capability of Molybdenum VI to Molybdenum V, which, under acidic pH, further reacts with phosphate and forms a green-colored complex. The intensity of the complex was measured spectrophotometrically at 695 nm, and TAC concerning a standard antioxidant, Vitamin C, was determined.

2.8. Triglyceride Estimation

The triglyceride levels in the flies were measured as per the protocol using a commercial kit based on the glycerol 3-phosphate oxidase-peroxidase method (Tulip Diagnostics (P) Ltd., Goa, India).

2.9. Glucose Estimation

The glucose content in the fly samples was measured as per the protocol based on the glucose oxidase-peroxidase method using a commercial kit (Agappe Diagnostics Ltd., Kerala, India).

2.10. Protein Estimation

The total protein content in control and CNS-treated (CNS500, CNS600, CNS700, CNS800, CNS900, and CNS1000) flies was estimated using Bradford reagent at 595 nm, using bovine serum albumin (Sigma-Aldrich, India) as the reference standard [34].

3. Results

3.1. Morphology and Structure of CNSs

The carbonization temperature was found to have a marked influence on the morphology of CNSs. As the pyrolysis temperature was increased from 500 to 1000 $^{\circ}$ C, a reduction in particle size was observed (Figure 1A–F), along with the formation of well-developed, spherical, solid carbon aggregates, which is the characteristic feature when the pyrolysis technique is used for the synthesis of carbon particles. The longer duration of synthesis time and controlled cooling rate could be responsible for the formation of spherical-shaped porous carbon nanomaterials.

Elemental composition was analyzed via EDS (Figure 2A). As the temperature increased from 500 to 1000 $^{\circ}$ C, the carbon content was enriched from \sim 74 to \sim 90% (Table 1). The carbon matrix was also embedded with self-doped oxygen, which continued to decrease in atomic percentage composition from CNS500 to CNS1000 from \sim 20% to \sim 8%, respectively. The CNSs also exhibited the presence of numerous alkali metals such as Na, Mg, K, and Ca, which were found to be present in trace quantities.

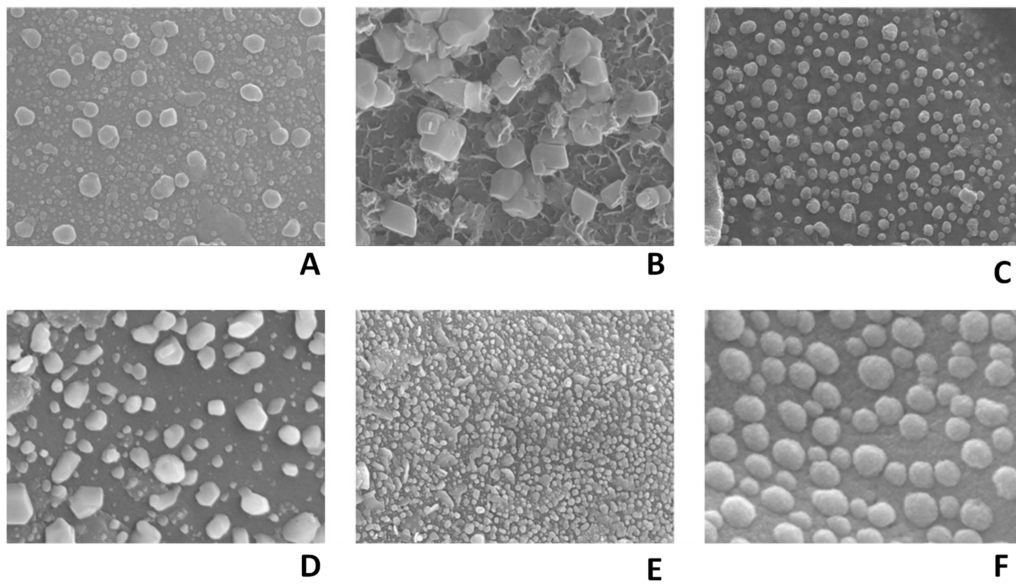


Figure 1. FESEM images of CNS500 (60 K \times) (A), CNS600 (50 K \times) (B), CNS700 (50 K \times) (C), CNS800 (50 K \times) (D), CNS900 (30 K \times) (E), and CNS1000 (150 K \times) (F).

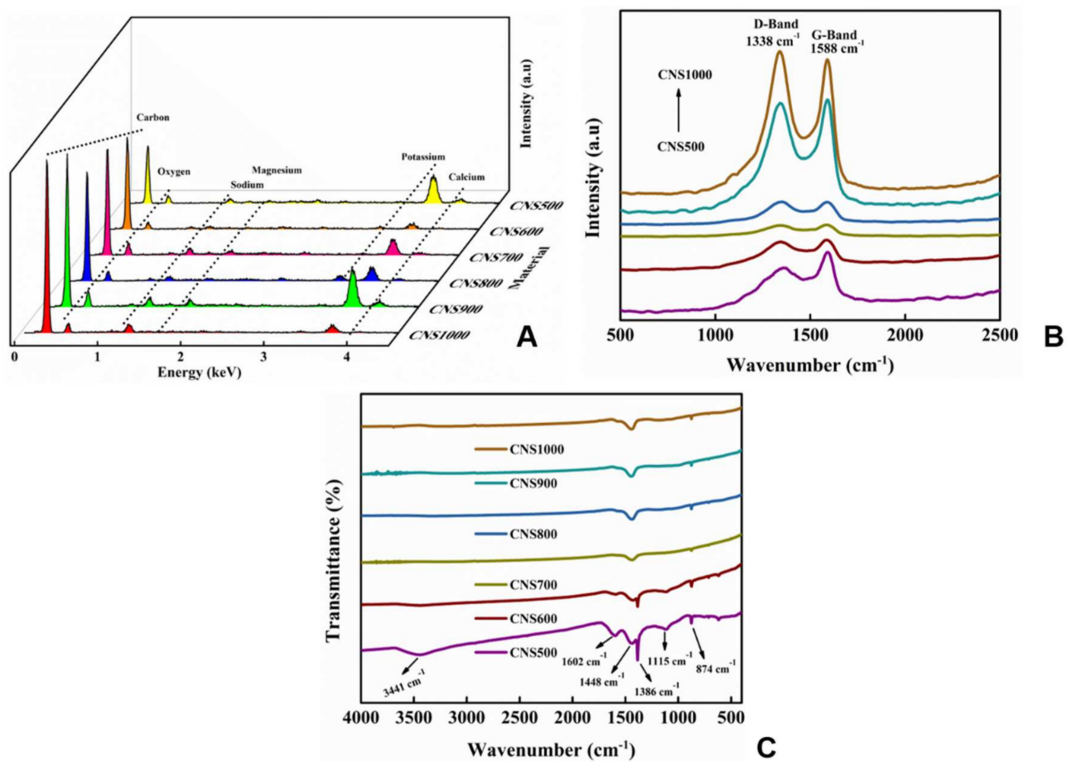


Figure 2. EDS spectra (A), Raman spectra (B), and FTIR spectra (C) of CNS500, CNS600, CNS700, CNS800, CNS900, and CNS1000 CNSs.

Table 1. Elemental composition (Atomic %) of ON CNSs.

CNSs	Carbon (C)	Oxygen (O)	Sodium (Na)	Magnesium (Mg)	Sulfur (S)	Potassium (K)	Calcium (Ca)
	Atomic Percentage (%)						
CNS500	74.2	19.4	0.5	0.8	0.2	0.9	4.0
CNS600	78.9	17.6	0.7	0.5	-	0.5	1.8
CNS700	87.2	10.9	-	0.2	-	1.0	0.7
CNS800	84.6	8.8	-	0.4	-	2.0	4.2
CNS900	89.5	9.9	-	-	-	0.6	-
CNS1000	90.7	8.6	-	-	-	0.7	-

CNSs were further analyzed for their structural features using Raman spectroscopy. The CNSs exhibited two prominent peaks (Figure 2B) at ~ 1338 and ~ 1588 cm^{-1} corresponding to the D-band and G-band, respectively. The D-band corresponds to vibrations of carbon atoms for in-plane terminations of disordered graphite, indicating disorder in the carbon structure. The G-band signifies the E_{2g} mode of graphite, which could be related to the vibration of sp^2 -bonded carbon atoms in a hexagonal lattice, indicating structural order. The relative intensities of the D-band and G-band (I_d/I_g) provide an index to assess the graphitic nature of carbon materials [7,35]. It was found that as the synthesis temperature was increased, the I_d/I_g value increased, suggesting the presence of more defective sites in CNS1000 ($I_d/I_g = 1.1$). This could be due to the greater fragmentation of the particles, creating edges at high temperatures. The liberation of gases such as H_2O , CO , and CO_2 at elevated temperatures further creates pores in the carbon residue, which contributes to the increased intensity of the D-band. Figure 2C shows the presence of functional groups assessed from FTIR spectra. A broad peak at ~ 3441 cm^{-1} indicates the presence of an intermolecularly bonded alcoholic or carboxylic acid $-OH$ group [36]. As the synthesis temperature was increased, the intensity of the peak decreased and disappeared for higher CNSs, suggesting the consumption or removal of the $-OH$ group from the biomass. $C=C$ stretching in carbon was detected by a peak at ~ 1602 cm^{-1} , which is also similar to $-OH$ group decreases in intensity [37]. $-C-H$ bending vibrations were detected by a peak at ~ 1448 cm^{-1} , which became more resolved at higher temperatures. $S=O$ stretching was also observed at ~ 1386 cm^{-1} . The presence of sulfur was also confirmed from the elemental analysis (EDS). However, the peak disappeared after CNS600, suggesting the removal of sulfur as oxides during pyrolysis progression towards higher temperatures. $-C-O$ stretching was also found at ~ 1115 cm^{-1} , which was also found to disappear at higher synthesis conditions, suggesting that it could have arisen from a secondary alcohol. Further $-C-H$ bending was detected at ~ 874 cm^{-1} , which could be attributed to the trisubstituted aromatic system, which remained throughout the CNS series and could have been responsible for some order in the carbon matrix [38,39].

The porosity of the CNSs was analyzed from N_2 adsorption/desorption isotherms. The specific surface area and pore volume were determined using the Brunauer–Emmett–Teller (BET) method, while the pore width was obtained from Barrett, Joyner, and Halenda (BJH) calculations (Figure 3). As the carbonization temperature was increased from 500 to 1000 $^{\circ}\text{C}$, the BET SSA was increased from ~ 6.2 to ~ 2960 m^2/g (Figure 3A). This could be attributed to the formation of porous structures and a reduction in the size of the particles with the increase in temperature, which provides an enhanced surface area [40]. As discussed earlier, a hierarchical porous structure within the carbon matrix is formed due to self-activation, facilitated by the presence of alkali metals that play a primary role in obtaining carbon residues with a large surface area [39]. Similarly, the pore volume was also increased from 0.009 cm^3 to 2.1 cm^3/g (Figure 3B). However, the pore width did not exhibit any specific order (Figure 3B). All the CNSs were found to be mesoporous (pore diameter = 2 to 50 nm).

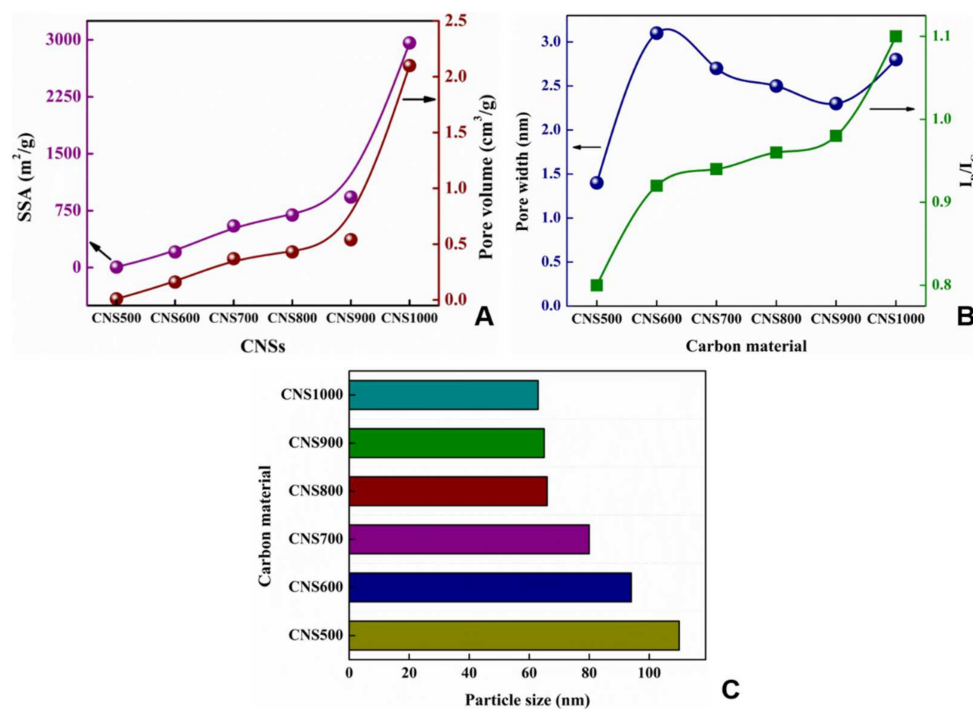


Figure 3. BET specific surface area and pore volume (A), pore width and I_D/I_G (B), and particle sizes of different carbon materials (C).

3.2. Toxicological Assay

To assess the chronic oral toxicity of mesoporous carbon nanoparticles synthesized from waste onion peel, a survival assay was performed with newly hatched male (Figure 4) and female (Figure 5) flies. The flies were fed with different doses (10, 100, and 1000 $\mu\text{g}/\text{mL}$) of CNS500 (Figures 4A and 5A), CNS600 (Figures 4B and 5B), CNS700 (Figures 4C and 5C), CNS800 (Figures 4D and 5D), CNS900 (Figures 4E and 5E), and CNS1000 (Figures 4F and 5F) CNSs and observed for a period of 25 days. The male flies treated with CNS500, CNS600, CNS700, CNS800, CNS900, and CNS1000 nanoparticles at the 10 $\mu\text{g}/\text{mL}$ dose did not show a significant difference in survival compared to control flies. However, male flies treated with 100 $\mu\text{g}/\text{mL}$ of nanoparticles showed a difference in the survival curve for CNS500 (Figure 4A) and CNS600 (Figure 4B) CNSs, respectively. Similarly, male flies treated with 1000 $\mu\text{g}/\text{mL}$ of nanoparticles showed a significant difference in survival rate for CNS500 (Figure 4A), CNS600 (Figure 4B), CNS800 (Figure 4D), and CNS900 (Figure 4E) CNSs, respectively. In female flies, only CNS500-treated flies showed a significant difference in survival rate for 100 and 1000 $\mu\text{g}/\text{mL}$ (Figure 5B) concentrations. However, at the 10 $\mu\text{g}/\text{mL}$ dose, they survived as compared to the control flies. Other nanoparticles, i.e., CNS600 (Figure 5b), CNS700 (Figure 5C), CNS800 (Figure 5D), CNS900 (Figure 5E), and CNS1000 (Figure 5F), showed no significant difference in survival rate at 10, 100, and 1000 $\mu\text{g}/\text{mL}$ concentrations, respectively. In summary, the survival curves for the control and CNS-treated groups did not exhibit any major difference among male and female flies (Figures 4 and 5). Based on these findings regarding the survival rate, all other biochemical and behavioral assays in adult males and females were performed after 25 days of exposure to the respective nanoparticles.

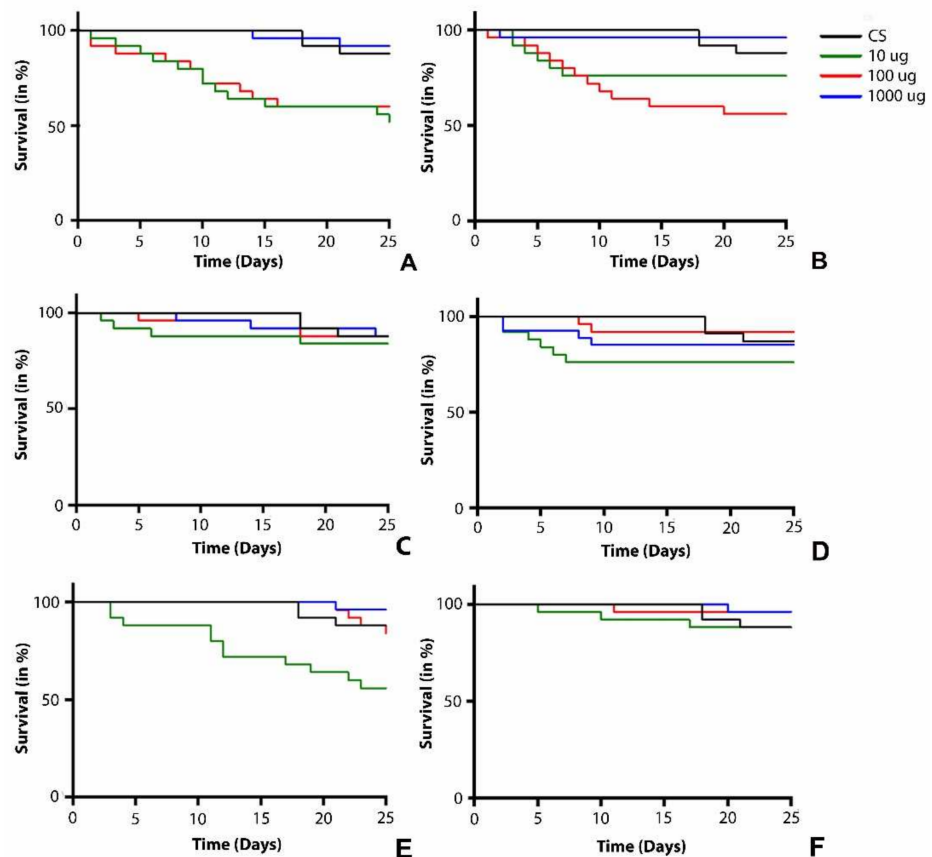


Figure 4. Survival assay curve of male flies treated with mesoporous carbon nanoparticles (A) CNS500, (B) CNS600, (C) CNS700, (D) CNS800, (E) CNS900, and (F) CNS1000 at 10, 100, and 1000 $\mu\text{g}/\text{mL}$ doses, respectively. Here, the black curve represents the survival rate of control flies. The blue, red, and green curves represent the survival rates of male flies at 10, 100, and 1000 $\mu\text{g}/\text{mL}$ doses, respectively.

The negative geotaxis or climbing assay was performed independently for males and females. In all CNS-treated groups (CNS500, CNS600, CNS700, CNS800, CNS900, and CNS1000), since there was no significant difference in the survival of both male and female flies for most of the nanoparticle concentrations tested, only the flies treated with the highest concentration of CNSs were considered for the negative geotaxis or climbing assay. The percentages of male flies that were able to cross the 20 cm mark in one minute (three times/vial and three food vials per dose) in control and CNS-treated (CNS500, CNS600, CNS700, CNS800, CNS900, and CNS1000) groups were 95, 77.8, 78.8, 77.8, 78.8, 87, and 80.6, respectively (Figure 6A). Similarly, the percentages of female flies that were able to cross the expected mark in one minute in the control and CNS-treated (CNS500, CNS600, CNS700, CNS800, CNS900, and CNS1000) groups were 91.7, 81, 84.6, 63, 83, 94.9, and 82, respectively (Figure 6B). Only female flies in the CNS700-treated group showed slight difficulty in climbing. However, in all other treated groups, both male and female flies showed no statistically significant difference compared to the control group.

The acetylcholinesterase (AChE) activity was estimated in male and female flies in response to dietary exposure of CNS500, CNS600, CNS700, CNS800, CNS900, and CNS1000 CNSs at a 1000 $\mu\text{g}/\text{mL}$ dose. The analysis revealed no significant difference between control and treatment groups, suggesting that 25 days of dietary exposure to mesoporous carbon nanoparticles did not elicit major neurotoxicity (Figure 7).

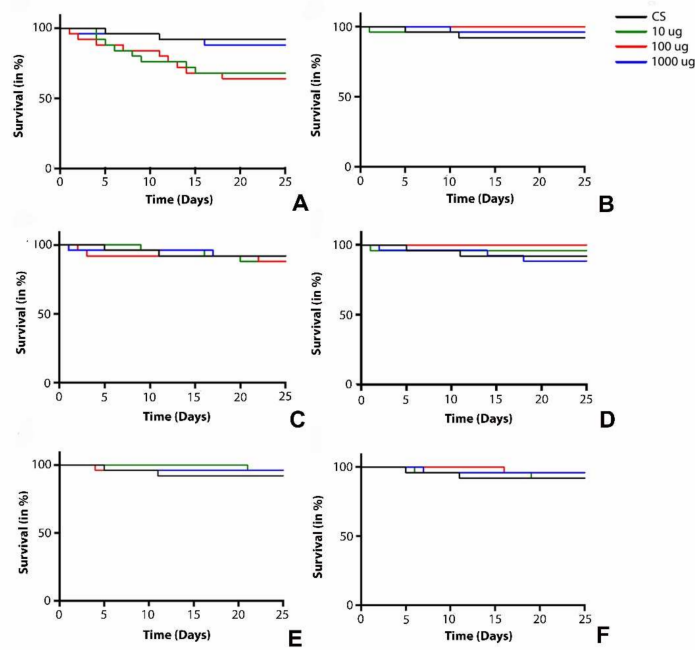


Figure 5. Survival assay curve of female flies treated with mesoporous carbon nanoparticles (A) CNS500, (B) CNS600, (C) CNS700, (D) CNS800, (E) CNS900, and (F) CNS1000 at 10, 100, and 1000 µg/mL doses, respectively. Here, the black curve represents the survival rate of control flies. The blue, red, and green curves represent the survival rates of female flies at 10, 100, and 1000 µg/mL doses, respectively.

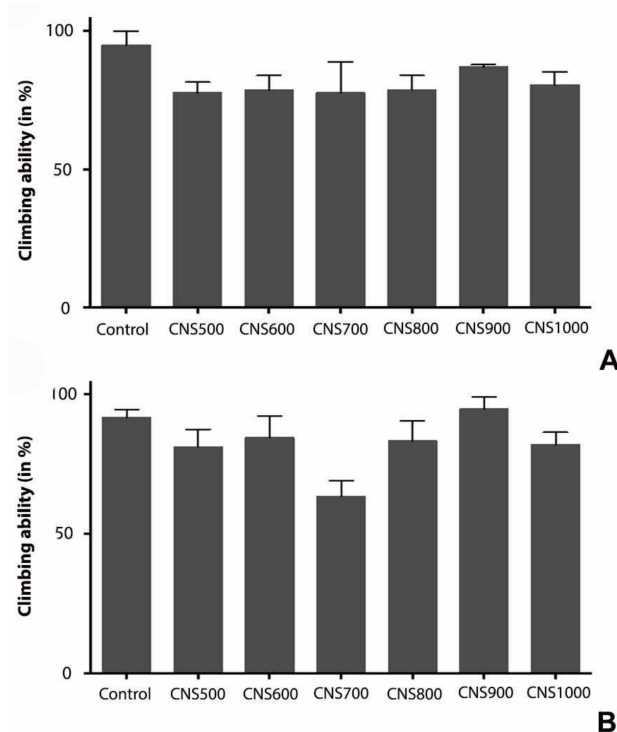


Figure 6. Negative geotaxis or climbing assay in carbon-nanoparticle-treated (A) male and (B) female flies. Both male (A) and female (B) flies were tested for their negative geotaxis behavior after 25 days of carbon nanoparticle treatment at 1000 µg/mL dose. The values represented are mean ± SEM and statistical significance was set at $p < 0.05$ when compared to control ($n = 3$ and 25 flies per treatment and control group).

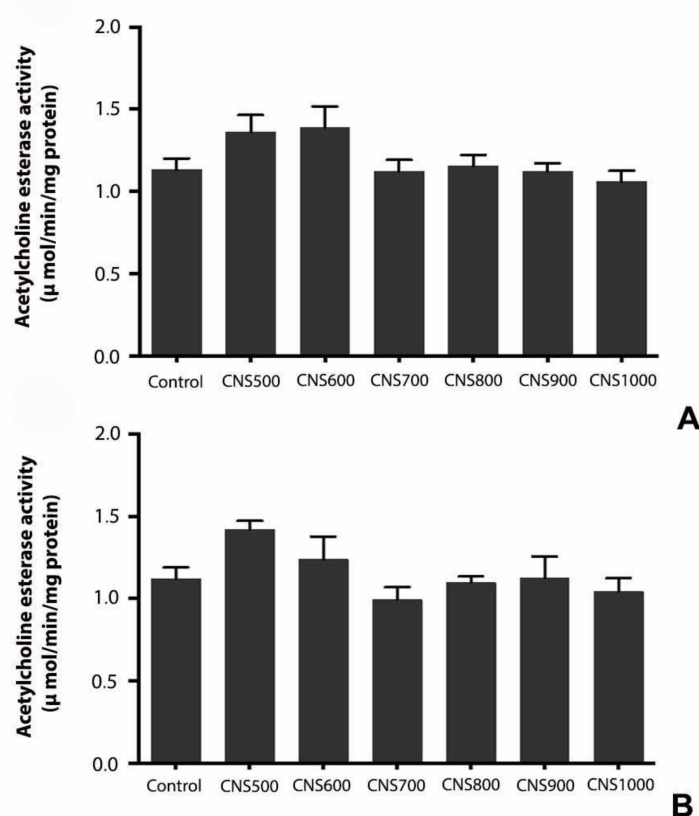


Figure 7. Estimation of acetylcholine esterase (AChE) activity in response to dietary exposure to CNS500, CNS600, CNS700, CNS800, CNS900, and CNS1000 CNSs for 25 days at 1000 $\mu\text{g}/\text{mL}$ in (A) male and (B) female flies. AChE activity was estimated using Ellman's method and values are represented as mean \pm SEM; statistical significance was set at $p < 0.05$ when compared to control ($n = 3$ and 25 flies per treatment group).

The continuous exposure of animals to toxic chemicals or nanoparticles is likely to induce oxidative stress due to the increased production of reactive oxidative species (ROS) or free radicals. The free radical scavenging or antioxidants can reverse the effect of ROS and thus their production in the animals can be used as a measure to quantify the level of oxidative stress [26]. The measurement of total antioxidant capacity (TAC) by the phosphomolybdenum method [33] after 25 days of exposure to CNS500, CNS600, CNS700, CNS800, CNS900, and CNS1000 mesoporous CNSs at a 1000 $\mu\text{g}/\text{mL}$ dose did not show statistically significant changes compared to controls, suggesting that CNSs did not elicit any oxidative stress at the organism level (Figure 8).

The effect of mesoporous CNS ingestion on the metabolic activities in flies was studied by estimating triglycerides, glucose, and protein levels. It was previously reported that exposure to silver nanoparticles at higher doses affected the energy reserves in flies, such as glycogen and protein, due to altered feeding behavior [41]. To test any metabolic changes or influence on the energy reserves in flies, the triglyceride, glucose, and protein content in those exposed to CNS500, CNS600, CNS700, CNS800, CNS900, and CNS1000 mesoporous CNSs at 1000 $\mu\text{g}/\text{mL}$ for 25 days was estimated. The experimental results revealed that there was no significant change in triglyceride (Figure 9), glucose (Figure 10), or protein (Figure 11) levels as compared to controls.

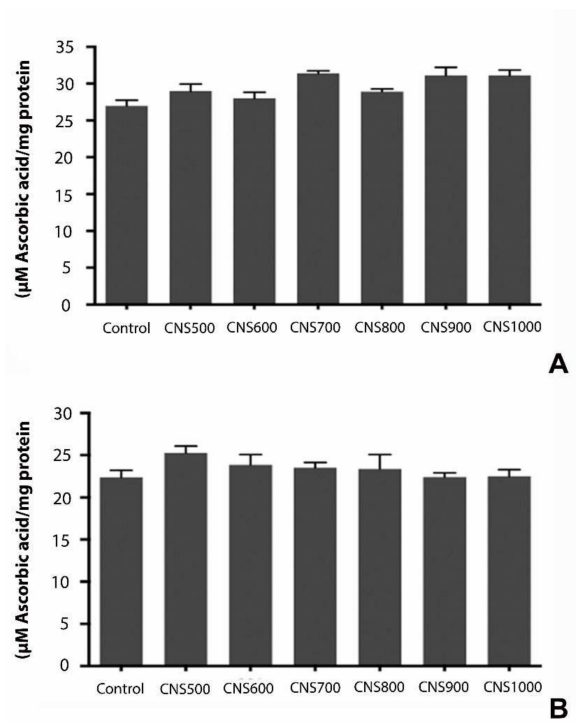


Figure 8. Estimation of total antioxidant capacity (TAC) in response to dietary exposure to CNS500, CNS600, CNS700, CNS800, CNS900, and CNS1000 CNSs for 25 days at 1000 µg/mL dose in (A) male and (B) female flies. TAC was estimated using the phosphomolybdenum method and values are represented as mean ± SEM; statistical significance was set at $p < 0.05$ when compared to control (n = 3 and 25 flies per treatment group).

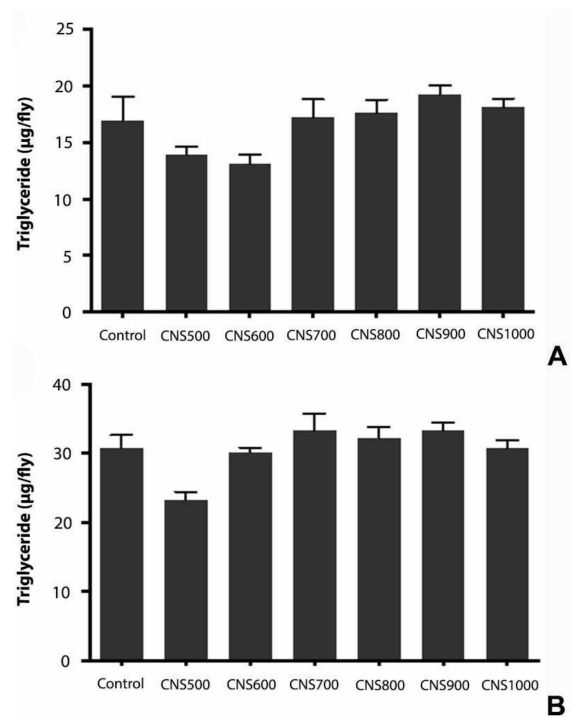


Figure 9. Estimation of triglycerides in response to dietary exposure to CNS500, CNS600, CNS700, CNS800, CNS900, and CNS1000 CNSs for 25 days at 1000 µg/mL dose in (A) male and (B) female flies. The values are represented as mean ± SEM and statistical significance was set at $p < 0.05$ when compared to control (n = 3 and 25 flies per treatment group).

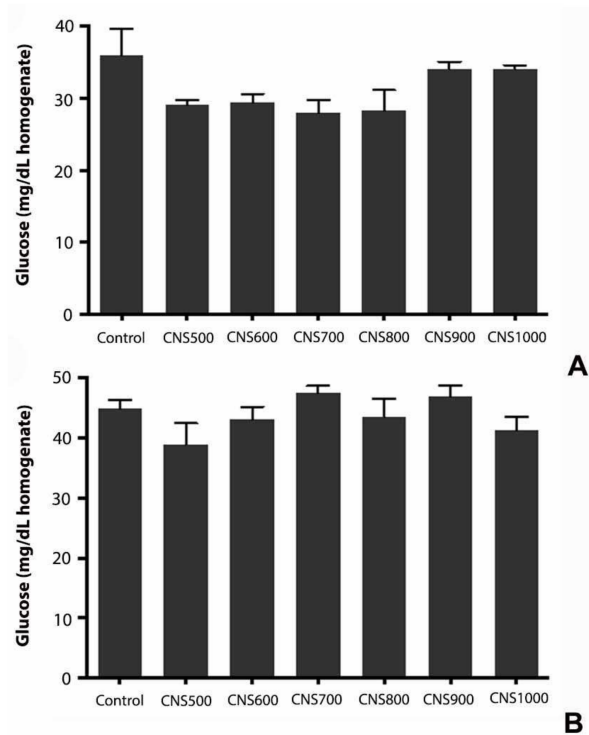


Figure 10. Estimation of glucose in response to dietary exposure to CNS500, CNS600, CNS700, CNS800, CNS900, and CNS1000 CNSs for 25 days at 1000 µg/mL dose in (A) male and (B) female flies. The values are represented as mean ± SEM and statistical significance was set at $p < 0.05$ when compared to control (n = 3 and 25 flies per treatment group).

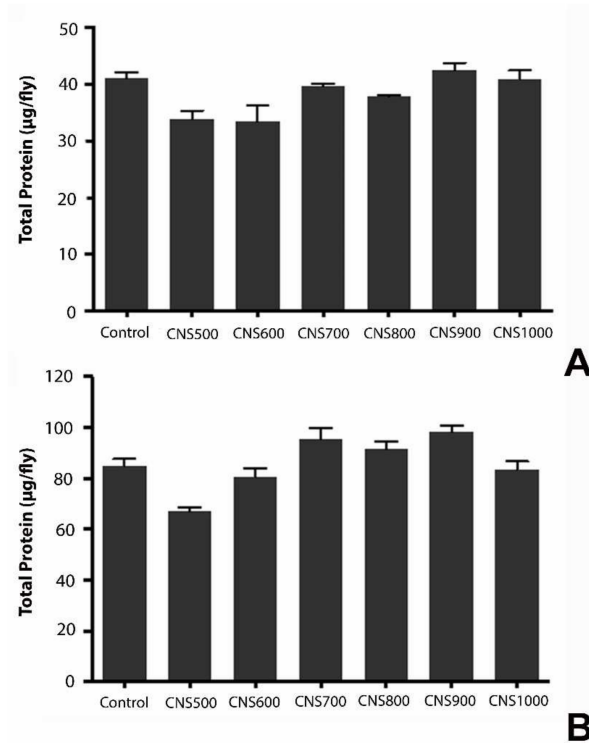


Figure 11. Estimation of protein in response to dietary exposure to CNS500, CNS600, CNS700, CNS800, CNS900, and CNS1000 CNSs for 25 days at 1000 µg/mL dose in (A) male and (B) female flies. The values are represented as mean ± SEM and statistical significance was set at $p < 0.05$ when compared to control (n = 3 and 25 flies per treatment group).

4. Discussion

Synthesized CNSs have been tested for various applications, such as electrode materials for energy storage devices and electrochemical sensors [37,42], in photomechanical actuators [43], and as materials for CO₂ adsorption [44], owing to the very high surface area and porosity. Such varied and increased use of nanoparticles leads to the exposure of humans to nanoparticles. Therefore, it is highly necessary to investigate the toxic effects elicited by such nanoparticles and various other nanomaterials and to determine the non-toxic dose for practical or safe applications. There are many studies investigating the toxic effect of carbon nanoparticles on the biological system [45–47].

In the present study, the toxicity of mesoporous CNSs synthesized from waste onion peel was evaluated using *Drosophila melanogaster* as an in vivo animal model. The mesoporous CNSs used in the current analysis have not been evaluated previously for their toxic effects using an in vivo model system. The present study's overall results highlight the non-toxic nature and beneficial impacts of mesoporous carbon nanoparticles at 1, 10, and 100 µL/mL doses.

The feeding of oral magnetite nanoparticles in *Drosophila* caused developmental changes, with a delay in egg to pupae and pupae to adult transformations [48]. Therefore, to assess the effect of mesoporous CNSs on the development of *Drosophila*, all the developmental stages were carefully analyzed. The larvae from the control and the treated groups at different concentrations reached different developmental stages such as larva, pupa, and adult on the same day. Thus, the oral administration of mesoporous carbon nanoparticles does not elicit any developmental delay in *Drosophila*.

The negative geotaxis or climbing assay was performed to assess the physiological impact of carbon nanoparticles on the motor system. Normally, flies tend to climb upwards when they are offered freedom to move vertically, and this can also be used to assess the neurodegeneration phenotype [26,49,50]. In the current analysis, the absence of significant changes in the climbing activity in CNS-nanoparticle-treated flies compared to control flies suggests that the oral administration of CNSs for 25 days did not cause any physiological/motor or neurodegenerative defects.

Neurotoxicity refers to the structural and functional changes in the neurons and glial cells in the central and peripheral nervous systems. The AChE assay is used to evaluate the activity of AChE, an enzyme that hydrolyzes acetylcholine to choline and acetic acid, and this analysis has been previously used to assess the neurotoxic potential of NPs in *Drosophila* [51,52]. The current results of the AChE analysis upon oral exposure to CNSs for 25 days did not reveal any significant changes in the activity of the enzyme. This suggests the absence of neurotoxicity upon dietary administration of CNSs at different concentrations. The effect of CNS ingestion on the metabolic activities in *Drosophila* was studied. It was previously reported that the ingestion of silver NPs at higher concentrations affected the energy reserves in flies, such as glycogen and protein. It also altered the feeding behavior in flies [41]. To test whether oral ingestion of CNSs for 25 days affected the energy reserves and feeding behavior in flies, the glucose, protein, and triglyceride content were estimated. There was no significant change in the glucose, protein, and triglyceride levels in flies. The results suggest that CNSs can be used to obtain beneficial effects in animals. The non-toxic nature of the synthesized mesoporous carbon nanomaterials in low concentrations could be due to their highly porous nature. Earlier research on functionalized CNTs has indicated a reduction in the toxicity of nanomaterials upon functionalization. This has been attributed to the formation of more defects within the system during the preparation of functionalized CNTs [20]. Raman spectroscopy results of the CNSs in the present research also show an increased I_D/I_G ratio with an increase in carbonization temperature, suggesting the development of defects throughout the carbon residue (CNSs). This could be one of the reasons for the low toxicity of CNSs. It has been reported earlier that water-soluble functionalized CNTs are less toxic compared to insoluble CNTs [53]. From the FTIR spectra, it is evident that the CNSs have —COOH groups mimicking acid-functionalized carbon nanomaterials. Recent studies have also

highlighted that the presence of metal impurities in CNTs induces enhanced toxicity compared to metal-free CNTs [13]. EDS spectra of CNSs show very low concentrations of metal impurities. The obtained characterization results for CNSs corroborate well with the results obtained from in vivo toxicological assays. The present research successfully highlights a method to synthesize low-cost, low-toxicity, porous carbon nanomaterials that can be used in wide applications.

5. Conclusions

Mesoporous CNSs were synthesized from waste onion peels using the pyrolysis technique at various temperatures (500–1000 °C). As-synthesized materials were characterized and were found to exhibit a very high specific surface area (SSA) of 2960 m²/g. The toxicity of CNSs was evaluated using *Drosophila melanogaster* as an in vivo animal model. The survival assay was carried out with freshly hatched male and female flies fed with different doses of CNSs synthesized at different carbonization temperatures. The survival curves for control and CNS-treated groups did not show any significant variation in both male and female flies. The negative geotaxis was performed independently for males, and female flies indicated no physiological neurodegenerative defects when compared with control groups. The CNSs did not elicit significant neurotoxicity, which was confirmed by the estimation of acetylcholine esterase. The experimental results did not exhibit a significant change in triglyceride, glucose, and protein levels compared to controls over 25 days in both male and female flies, suggesting that CNSs did not significantly affect metabolic activities. The lower or less toxic effects of CNSs in an in vivo genetic model such as *Drosophila melanogaster* support their possible use in biological applications such as drug carriers and others.

Author Contributions: Formal analysis, investigation, writing—original draft preparation, V.S.B. and A.K.K.; Resources, data curation, H.V.N. and R.G.; Conceptualization, methodology, visualization, supervision, P.D.P., S.V.R. and G.H. All authors have read and agreed to the published version of the manuscript.

Funding: This research did not receive any specific grant from funding agencies in the public, commercial, or not-for-profit sectors.

Institutional Review Board Statement: Not applicable (All experiments related to fruit fly (*Drosophila melanogaster*) were carried out under the U.K. Animals (Scientific Procedures) Act, 1986, and other globally accepted standards were followed and maintained).

Informed Consent Statement: Not applicable.

Data Availability Statement: The data are contained within the article itself. Specific data regarding any studies are available on request from the corresponding author.

Acknowledgments: One of the authors, Shamprasad Varija Raghu, acknowledges support from the DBT-Ramalingaswami Re-Entry Fellowship (102/IFD/SAN/1997/2015-16).

Conflicts of Interest: The authors declare no conflict of interest.

References

1. Pierson, H.O. (Ed.) 2—The Element Carbon. In *Handbook of Carbon, Graphite, Diamonds and Fullerenes*; William Andrew Publishing: Oxford, UK, 1993; pp. 11–42.
2. Lozano-Castello, D.; Lillo-Rodenas, M.A.; Cazorla-Amoros, D.; Linares-Solano, A. Preparation of activated carbons from Spanish anthracite: I. Activation by KOH. *Carbon* **2001**, *39*, 741–749. [[CrossRef](#)]
3. Hegde, G.; Manaf, S.A.A.; Kumar, A.; Ali, G.A.M.; Chong, K.F.; Ngaini, Z.; Sharma, K.V. Biowaste Sago Bark Based Catalyst Free Carbon Nanospheres: Waste to Wealth Approach. *ACS Sustain. Chem. Eng.* **2015**, *3*, 2247–2253. [[CrossRef](#)]
4. Pumera, M.; Ambrosi, A.; Bonanni, A.; Chng, E.L.K.; Poh, H.L. Graphene for electrochemical sensing and biosensing. *TrAC Trends Anal. Chem.* **2010**, *29*, 954–965. [[CrossRef](#)]
5. Soboleva, T.; Zhao, X.; Malek, K.; Xie, Z.; Navessin, T.; Holdcroft, S. On the Micro-, Meso-, and Macroporous Structures of Polymer Electrolyte Membrane Fuel Cell Catalyst Layers. *ACS Appl. Mater. Interfaces* **2010**, *2*, 375–384. [[CrossRef](#)] [[PubMed](#)]

6. Xu, B.; Chen, Y.; Wei, G.; Cao, G.; Zhang, H.; Yang, Y. Activated carbon with high capacitance prepared by NaOH activation for supercapacitors. *Mater. Chem. Phys.* **2010**, *124*, 504–509. [[CrossRef](#)]
7. Nieto-Márquez, A.; Romero, R.; Romero, A.; Valverde, J.L. Carbon nanospheres: Synthesis, physicochemical properties and applications. *J. Mater. Chem.* **2011**, *21*, 1664–1672. [[CrossRef](#)]
8. Bhat, V.S.; Supriya, S.; Hegde, G. Biomass Derived Carbon Materials for Electrochemical Sensors. *J. Electrochem. Soc.* **2020**, *167*, 037526. [[CrossRef](#)]
9. Vix-Guterl, C.; Frackowiak, E.; Jurewicz, K.; Friebe, M.; Parmentier, J.; Béguin, F. Electrochemical energy storage in ordered porous carbon materials. *Carbon* **2005**, *43*, 1293–1302. [[CrossRef](#)]
10. Zhai, Y.; Dou, Y.; Zhao, D.; Fulvio, P.F.; Mayes, R.; Dai, S. Carbon Materials for Chemical Capacitive Energy Storage. *Adv. Mater.* **2011**, *23*, 4828–4850. [[CrossRef](#)]
11. Wang, Y.; Sun, Z.; Chen, Z. Energy management strategy for battery/supercapacitor/fuel cell hybrid source vehicles based on finite state machine. *Appl. Energy* **2019**, *254*, 113707. [[CrossRef](#)]
12. Li, Z.; Guo, D.; Liu, Y.; Wang, H.; Wang, L. Recent advances and challenges in biomass-derived porous carbon nanomaterials for supercapacitors. *Chem. Eng. J.* **2020**, *397*, 125418. [[CrossRef](#)]
13. Yuan, X.; Zhang, X.; Sun, L.; Wei, Y.; Wei, X. Cellular Toxicity and Immunological Effects of Carbon-based Nanomaterials. *Part. Fibre Toxicol.* **2019**, *16*, 18. [[CrossRef](#)]
14. Kobayashi, N.; Izumi, H.; Morimoto, Y. Review of toxicity studies of carbon nanotubes. *J. Occup. Health* **2017**, *59*, 394–407. [[CrossRef](#)] [[PubMed](#)]
15. Shvedova, A.; Castranova, V.; Kisin, E.; Schwegler-Berry, D.; Murray, A.; Gandelsman, V.; Maynard, A.; Baron, P. Exposure to Carbon Nanotube Material: Assessment of Nanotube Cytotoxicity using Human Keratinocyte Cells. *J. Toxicol. Environ. Health Part A* **2003**, *66*, 1909–1926. [[CrossRef](#)]
16. Wan, B.; Wang, Z.-X.; Lv, Q.-Y.; Dong, P.-X.; Zhao, L.-X.; Yang, Y.; Guo, L.-H. Single-walled carbon nanotubes and graphene oxides induce autophagosome accumulation and lysosome impairment in primarily cultured murine peritoneal macrophages. *Toxicol. Lett.* **2013**, *221*, 118–127. [[CrossRef](#)] [[PubMed](#)]
17. Cheng, C.; Müller, K.H.; Koziol, K.K.; Skepper, J.N.; Midgley, P.A.; Welland, M.E.; Porter, A.E. Toxicity and imaging of multi-walled carbon nanotubes in human macrophage cells. *Biomaterials* **2009**, *30*, 4152–4160. [[CrossRef](#)] [[PubMed](#)]
18. Sato, Y.; Yokoyama, A.; Shibata, K.-I.; Akimoto, Y.; Ogino, S.-I.; Nodasaka, Y.; Kohgo, T.; Tamura, K.; Akasaka, T.; Uo, M.; et al. Influence of length on cytotoxicity of multi-walled carbon nanotubes against human acute monocytic leukemia cell line THP-1 in vitro and subcutaneous tissue of rats in vivo. *Mol. BioSyst.* **2005**, *1*, 176–182. [[CrossRef](#)] [[PubMed](#)]
19. Fenoglio, I.; Aldieri, E.; Gazzano, E.; Cesano, F.; Colonna, M.; Scarano, D.; Mazzucco, G.; Attanasio, A.; Yakoub, Y.; Lison, D.; et al. Thickness of Multiwalled Carbon Nanotubes Affects Their Lung Toxicity. *Chem. Res. Toxicol.* **2011**, *25*, 74–82. [[CrossRef](#)]
20. Sweeney, S.; Hu, S.; Ruenraroengsak, P.; Chen, S.; Gow, A.; Schwander, S.; Zhang, J.; Chung, K.F.; Ryan, M.P.; Porter, A.E.; et al. Carboxylation of multiwalled carbon nanotubes reduces their toxicity in primary human alveolar macrophages. *Environ. Sci. Nano* **2016**, *3*, 1340–1350. [[CrossRef](#)]
21. Rydman, E.M.; Ilves, M.; Koivisto, A.J.; Kinaret, P.A.S.; Fortino, V.; Savinko, T.S.; Lehto, M.T.; Pulkkinen, V.; Vippola, M.; Hämeri, K.J.; et al. Inhalation of rod-like carbon nanotubes causes unconventional allergic airway inflammation. *Part. Fibre Toxicol.* **2014**, *11*, 48. [[CrossRef](#)]
22. Hsieh, W.-Y.; Chou, C.-C.; Ho, C.-C.; Yu, S.-L.; Chen, H.-Y.; Chou, H.-Y.E.; Chen, J.J.; Chen, H.-W.; Yang, P.-C. Single-Walled Carbon Nanotubes Induce Airway Hyperreactivity and Parenchymal Injury in Mice. *Am. J. Respir. Cell Mol. Biol.* **2012**, *46*, 257–267. [[CrossRef](#)] [[PubMed](#)]
23. Erdely, A.; Dahm, M.; Chen, B.T.; Zeidler-Erdely, P.C.; E Fernback, J.; Birch, M.E.; E Evans, D.; Kashon, M.L.; A Deddens, J.; Hulderman, T.; et al. Carbon nanotube dosimetry: From workplace exposure assessment to inhalation toxicology. *Part. Fibre Toxicol.* **2013**, *10*, 53. [[CrossRef](#)] [[PubMed](#)]
24. Vecchio, G.; Galeone, A.; Brunetti, V.; Maiorano, G.; Rizzello, L.; Sabella, S.; Cingolani, R.; Pompa, P.P. Mutagenic effects of gold nanoparticles induce aberrant phenotypes in *Drosophila melanogaster*. *Nanomed. Nanotechnol. Biol. Med.* **2012**, *8*, 1–7. [[CrossRef](#)] [[PubMed](#)]
25. Sabat, D.; Patnaik, A.; Ekka, B.; Dash, P.; Mishra, M. Investigation of titania nanoparticles on behaviour and mechanosensory organ of *Drosophila melanogaster*. *Physiol. Behav.* **2016**, *167*, 76–85. [[CrossRef](#)]
26. Sundararajan, V.; Dan, P.; Kumar, A.; Venkatasubbu, G.D.; Ichihara, S.; Ichihara, G.; Mohideen, S.S. *Drosophila melanogaster* as an in vivo model to study the potential toxicity of cerium oxide nanoparticles. *Appl. Surf. Sci.* **2019**, *490*, 70–80. [[CrossRef](#)]
27. El Kholly, S.; Giesy, J.P.; Al Nagggar, Y. Consequences of a short-term exposure to a sub lethal concentration of CdO nanoparticles on key life history traits in the fruit fly (*Drosophila melanogaster*). *J. Hazard. Mater.* **2021**, *410*, 124671. [[CrossRef](#)]
28. Pandey, U.B.; Nichols, C.D. Human disease models in *Drosophila melanogaster* and the role of the fly in therapeutic drug discovery. *Pharmacol. Rev.* **2011**, *63*, 411–436. [[CrossRef](#)]
29. Brand, A.H.; Perrimon, N. Targeted gene expression as a means of altering cell fates and generating dominant phenotypes. *Development* **1993**, *118*, 401–415. [[CrossRef](#)]
30. Raghu, S.V.; Mohammad, F.; Chua, J.Y.; Lam, J.S.W.; Loberas, M.; Sahani, S.; Barros, C.S.; Claridge-Chang, A. A zinc-finger fusion protein refines Gal4-defined neural circuits. *Mol. Brain* **2018**, *11*, 46. [[CrossRef](#)]

31. Raghu, S.V.; Patil, R. GAL4-UAS system for genetic labeling and visualization of specific regions of brain. In *Experiments with Drosophila for Biology Courses*; Indian Academy of Sciences: Bengaluru, India, 2021; pp. 233–237.
32. Ellman, G.L.; Courtney, K.D.; Andres, V., Jr.; Featherstone, R.M. A new and rapid colorimetric determination of acetylcholinesterase activity. *Biochem. Pharmacol.* **1961**, *7*, 88–95. [[CrossRef](#)]
33. Prieto, P.; Pineda, M.; Aguilar, M. Spectrophotometric Quantitation of Antioxidant Capacity through the Formation of a Phosphomolybdenum Complex: Specific Application to the Determination of Vitamin E. *Anal. Biochem.* **1999**, *269*, 337–341. [[CrossRef](#)]
34. Bradford, M.M. A rapid and sensitive method for the quantitation of microgram quantities of protein utilizing the principle of protein-dye binding. *Anal. Biochem.* **1976**, *72*, 248–254. [[CrossRef](#)]
35. Bhat, V.S.; Krishnan, S.G.; Jayeoye, T.J.; Rujiralai, T.; Sirimahachai, U.; Viswanatha, R.; Khalid, M.; Hegde, G. Self-activated ‘green’ carbon nanoparticles for symmetric solid-state supercapacitors. *J. Mater. Sci.* **2021**, *56*, 13271–13290. [[CrossRef](#)]
36. Kanagavalli, P.; Pandey, G.R.; Bhat, V.S.; Veerapandian, M.; Hegde, G. Nitrogenated-carbon nanoelectrocatalyst advertently processed from bio-waste of *Allium sativum* for oxygen reduction reaction. *J. Nanostruct. Chem.* **2021**, *11*, 343–352. [[CrossRef](#)]
37. Akshaya, K.B.; Bhat, V.S.; Varghese, A.; George, L.; Hegde, G. Non-Enzymatic Electrochemical Determination of Progesterone Using Carbon Nanospheres from Onion Peels Coated on Carbon Fiber Paper. *J. Electrochem. Soc.* **2019**, *166*, B1097–B1106.
38. Bhat, V.S.; Hegde, G.; Nasrollahzadeh, M. A sustainable technique to solve growing energy demand: Porous carbon nanoparticles as electrode materials for high-performance supercapacitors. *J. Appl. Electrochem.* **2020**, *50*, 1243–1255. [[CrossRef](#)]
39. Bhat, V.S.; Jayeoye, T.J.; Rujiralai, T.; Sirimahachai, U.; Chong, K.F.; Hegde, G.S. Acacia auriculiformis-Derived Bimodal Porous Nanocarbons via Self-Activation for High-Performance Supercapacitors. *Front. Energy Res.* **2021**, *519*. [[CrossRef](#)]
40. Supriya, S.; Sriram, G.; Ngaini, Z.; Kavitha, C.; Kurkuri, M.; De Padova, I.P.; Hegde, G. The Role of Temperature on Physical-Chemical Properties of Green Synthesized Porous Carbon Nanoparticles. *Waste Biomass Valorization* **2020**, *11*, 3821–3831. [[CrossRef](#)]
41. Raj, A.; Shah, P.; Agrawal, N. Sedentary behavior and altered metabolic activity by AgNPs ingestion in *Drosophila melanogaster*. *Sci. Rep.* **2017**, *7*, 15617. [[CrossRef](#)]
42. Ali, G.A.M.; Supriya, S.; Chong, K.F.; Shaaban, E.R.; Algarni, H.; Maiyalagan, T.; Hegde, G. Superior supercapacitance behavior of oxygen self-doped carbon nanospheres: A conversion of *Allium cepa* peel to energy storage system. *Biomass Convers. Biorefin.* **2019**, *11*, 1311–1323. [[CrossRef](#)]
43. Satapathy, P.; Adiga, R.; Kumar, M.; Hegde, G.; Prasad, S.K. Porous nanocarbon particles drive large magnitude and fast photomechanical actuators. *J. Nanostruct. Chem.* **2021**, *1–14*. [[CrossRef](#)]
44. Sriram, G.; Supriya, S.; Kurkuri, M.; Hegde, G. Efficient CO₂ adsorption using mesoporous carbons from biowastes. *Mater. Res. Express* **2019**, *7*, 015605. [[CrossRef](#)]
45. Pandey, H.; Saini, S.; Singh, S.P.; Gautam, N.K.; Singh, S. Candle soot derived carbon nanoparticles: An assessment of cellular and progressive toxicity using *Drosophila melanogaster* model. *Comp. Biochem. Physiol. Part C Toxicol. Pharmacol.* **2020**, *228*, 108646. [[CrossRef](#)] [[PubMed](#)]
46. Min, K.-J.; Lee, S.-H.; Lee, H.-Y.; Lee, E.-J.; Khang, D. Effects of carbon nanofiber on physiology of *Drosophila*. *Int. J. Nanomed.* **2015**, *10*, 3687–3697. [[CrossRef](#)]
47. Liu, X.; Vinson, D.; Abt, D.; Hurt, R.H.; Rand, D.M. Differential Toxicity of Carbon Nanomaterials in *Drosophila*: Larval Dietary Uptake Is Benign, but Adult Exposure Causes Locomotor Impairment and Mortality. *Environ. Sci. Technol.* **2009**, *43*, 6357–6363. [[CrossRef](#)]
48. Chen, H.; Wang, B.; Feng, W.; Du, W.; Ouyang, H.; Chai, Z.; Bi, X. Oral magnetite nanoparticles disturb the development of *Drosophila melanogaster* from oogenesis to adult emergence. *Nanotoxicology* **2015**, *9*, 302–312. [[CrossRef](#)]
49. Ali, Y.O.; Escala, W.; Ruan, K.; Zhai, R. Assaying Locomotor, Learning, and Memory Deficits in *Drosophila* Models of Neurodegeneration. *J. Vis. Exp.* **2011**, e2504. [[CrossRef](#)]
50. Linderman, J.A.; Chambers, M.C.; Gupta, A.S.; Schneider, D.S. Infection-Related Declines in Chill Coma Recovery and Negative Geotaxis in *Drosophila melanogaster*. *PLoS ONE* **2012**, *7*, e41907. [[CrossRef](#)]
51. Williamson, S.M.; Moffat, C.; Gomersall, M.A.E.; Saranzewa, N.; Connolly, C.N.; Wright, G.A. Exposure to Acetylcholinesterase Inhibitors Alters the Physiology and Motor Function of Honeybees. *Front. Physiol.* **2013**, *4*, 13. [[CrossRef](#)]
52. Siddique, Y.H.; Khan, W.; Fatima, A.; Jyoti, S.; Naz, F.; Singh, B.R.; Naqvi, A.H.; Haidari, M.; Khanam, S.; Ali, F.; et al. Toxic potential of copper-doped ZnO nanoparticles in *Drosophila melanogaster* (Oregon R). *Toxicol. Mech. Methods.* **2015**, *25*, 425–432. [[CrossRef](#)]
53. Sayes, C.M.; Liang, F.; Hudson, J.L.; Mendez, J.; Guo, W.; Beach, J.M.; Moore, V.C.; Doyle, C.D.; West, J.L.; Billups, W.E.; et al. Functionalization density dependence of single-walled carbon nanotubes cytotoxicity in vitro. *Toxicol. Lett.* **2006**, *161*, 135–142. [[CrossRef](#)] [[PubMed](#)]